

# Electrical resistivity tomography applied to detect contamination on a dairy farm in the Pampean region, Argentina

Claudia M. Sainato\*, Beatriz N. Losinno and Horacio J. Malleville

University of Buenos Aires, School of Agronomy, Physics Department, Av. San Martín 4453, C1417DSE, Buenos Aires, Argentina

Received July 2009, revision accepted December 2009

## ABSTRACT

On dairy farms, it is important to identify the degree of contamination that different management units, as localized sources, produce on soil and groundwater due to animal effluents. This information may be used to improve management practices in order to maintain not only environmental sustainability but also the standards of milk production. The aim was to test the performance of electrical resistivity tomography to detect anomalies of resistivity and to identify the relative impact, on physicochemical properties of soil and groundwater, produced by the effluents of the different management units of a dairy farm situated in the southern part of Santa Fe Province (Argentina). Twelve electrical resistivity tomography (ERT) profiles were carried out and 2D models of the resistivity distribution were interpreted together with the physicochemical analysis of soil and groundwater samples. At the plots around the milking house, resistivity decreased in the non-saturated zone between 60–84% relative to the background values, being the maximum value for the feeding zone, the most critical management unit, in agreement with sampling results. The surroundings of the lagoon of effluents showed a decrease of resistivity around 80%, even on the phreatic aquifer, due to flooding events in the past. Electrical resistivity tomography was sensitive enough to evaluate anomalies in the distribution of electrical conductivity associated with an increase of nitrates, sulphates and bicarbonates, in addition to phosphorous in soil and chlorides in groundwater, in all cases probably connected directly or indirectly with the animal waste.

## INTRODUCTION

It is widely known that intensive cattle activities produce effluents that may cause contamination of soil and groundwater. The main elements found in soils are nitrogen, from animal urine and manure and phosphorous because of its high concentration included in animal food (Herrero *et al.* 2006). Nitrates and chlorides have high mobility in soils and they may be found at greater depths.

Harter *et al.* (2002) found at dairies in California, with a semi-arid climate, that average shallow groundwater nitrate-N concentrations were almost three times greater than values at wells upgradient, although they did not significantly vary across dairy farm management units. Average electrical conductivity levels were twice the values immediately upgradient, being significantly higher in corral and pond areas indicating leaching from those management units. Pond leaching was further inferred from the presence of reduced nitrogen in three of four wells located immediately downgradient. Ullman and Mukhtar (2007) studied the impact of dairy practices on the characteristics of a

lagoon of effluents, concluding that salinity levels should be monitored to ensure adequate treatment of dairy farm waste and extend lagoon life expectancy.

In Argentina, Andriulo *et al.* (2003) found soil salinity and nitrates in groundwater at feedlots placed in the humid Pampean region. The southern part of Santa Fe Province (Argentina) is a plain with highly productive lands where there is a very important agricultural and cattle activity and a great number of dairy farms. Herrero *et al.* (2002) evaluated that the quality of the milk produced on farms in this zone was strongly correlated with the quality of groundwater used for animal drink. Therefore, it is necessary to maintain not only environmental sustainability but also the standards of milk production, identifying the degree of contamination that different management units produce as localized sources in order to improve management strategies.

Geophysical methods based on the study of electrical resistivity were proved to be very important in making a diagnosis of soil contamination by industrial and urban localized sources (Meju 2000). The advantage of these methods is a quick exploration, non-invasive and low cost, of the soil and groundwater at sites of localized sources of contamination

\* csainato@agro.uba.ar

that may require an exhaustive later sampling.

These methods have not been widely applied to contamination sources by intensive agricultural and cattle activities. Groundwater contamination by nitrates at dairies was studied by Drommerhausen *et al.* (1995) by means of the electromagnetic induction method determining the limits of the contaminated zone within the dairy farm. Sainato *et al.* (2006) found anomalous values of electrical conductivity below the corrals on a small dairy farm, in the humid Pampean region, using electrical resistivity soundings.

The aim of this work was to test the performance of electrical resistivity tomography to detect anomalies of conductivity due to the effluents of the different management units of a dairy farm situated in the southern part of Santa Fe Province (Argentina). The relative impact, produced by animal waste on the physico-chemical properties of soil and groundwater was also identified.

## MATERIAL AND METHODS

### Study zone

The dairy farm is situated in the town of Venado Tuerto (Santa Fe Province, Argentina), a zone characterized by a great number of cattle farms, belonging to the flat 'Chacoparanense' basin (Fig. 1). It is placed in a transitional zone between the so-called 'Rolling Pampa' and the 'Sandy Pampa'. The dairy farm is located between two level curves of 105 m a.s.l. at the E and W, while a low curve of 102.5 m a.s.l. is placed in the centre of the area. The climate in this zone is moderately mild (average annual temperature of 16.4 °C), with an average annual precipita-

tion of around 900 mm. The hydric balance shows a slight deficiency of water in summer due to evapotranspiration but the equilibrium is reached in autumn and winter, when an excess of humidity is encountered in the soil. However, events of flooding during periods of hard rain can not be disregarded. In fact there was a flood during 1994 and 2001 in this zone.

The soil is of sandy loamy type (INTA 1972) and there is no presence of a clayey horizon. The soils belong to the 'Santa Isabel' series, deep and well drained and they have evolved over loamy eolian sediments.

The soil profile shows the first 36 cm well supplied with organic matter (horizon A1). The lower horizon B2 has moderately high permeability with less clay than A1. At 95–100 cm depth, the soil has a lower consistency. The values of soil equivalent humidity are 16.5% for the first 20 cm, 21.7% from 20–36 cm and below it decreases up to 14.5% at 100 cm depth.

At the study zone runoff paths are not well-defined, mainly due to the smooth topography. The hydrological basin is endorheic – the exceeding volume of water is evaporated or infiltrates. When precipitation periods are long, the low zones and lagoons overflow. The farm is placed in a water parting area, with a very flat topography and where water is easily accumulated during rainy periods. The superficial drainage is oriented to the permanent lagoons in the region. Values of infiltration velocity were measured in these soils, showing a value of 6 mm/h, strongly correlated with organic matter content, the same order of magnitude as the saturated hydraulic conductivity (6.56 mm/h) (Rossi 2004).

The hydrogeological formations in the zone are (Palazzo *et al.* 2003): the Loess Pospampeano from surface up to a variable depth between 4–12 m, composed by clayey silt of Aeolian origin. Below, the Pampeano Formation is located, with a variable thickness around 60 m, constituted by clayey silt and fine sands. It contains the Pampeano aquifer, which is a sequence of permeable and less permeable levels constituting a multilayer aquifer (permeability around 4 m/d) and effective porosity of 10%. In its upper part, it includes the free groundwater level. The regional direction of groundwater flow is SW-NE (Fili *et al.* 1999) and locally it may follow the topography. Underlying, the Puelche Formation is composed of sands with good permeability and fluvial origin. It is separated from the Pampeano by an aquitard 8 m thick. The recharge of the aquifers is autochthon and direct.

### Dairy farm management

The dairy farm has a surface of 260 ha and it is divided into 7 plots for agriculture and cattle. There are 230 cows with a production rate of 3080 l per day. There is a residence located at 1000 m to the east of the milking house and an adjacent corral for confinement. There was a great flood in 2001 that affected the residence and the plot located at the north of it, as seen in Fig. 1. These plots are devoted to agriculture at the moment.

The animals are moved, after milking, to a plot at the southern part of the dairy farm where they stay for feeding and afterwards

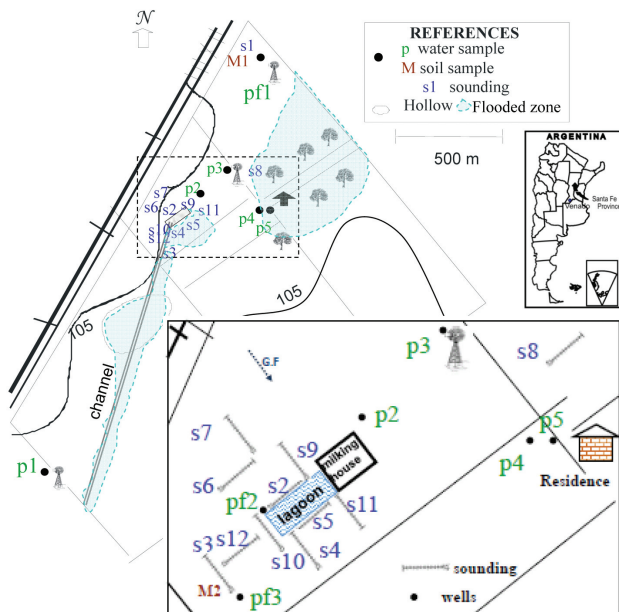


FIGURE 1 Map of the dairy farm with topography, location of geoelectrical soundings, wells and soil sampling sites. Zones of floods in 1994 and 2001 are outlined. Arrow G.F. shows the approximate direction of groundwater flow (Fili *et al.* 1999).

they are lead to the pasture plots. At the milking house, water is obtained from well p2, which is 12 m deep and it is used for the cleaning of the milking machine and animals. The manure is cleaned with water that runs off up to the limits of the corral.

All these effluents from the milking house and the corral are driven into a channel that connects to a lagoon (Fig. 1). Beyond the lagoon, the channel continues to the SW towards the pond. The lagoon of effluents overflowed towards its eastern and southern side in 2001.

### Electrical resistivity tomography

A systematic distribution of soundings was performed, in a gradient manner, following the guides for environmental studies (IHOBE 2003). The soundings were located along the intended direction of maximum variation of electrical conductivity, taking into account the morphology of the surface (topography). This would be probably associated with the superficial runoff of the effluents and the direction of groundwater flow, which in this area corresponds to decreasing topography (in this case towards the centre of the dairy farm where there is a pond).

Twelve electrical resistivity tomography (ERT) profiles were carried out using a SARIS resistivitymeter (Scintrex) of 100 W output power. The number of cycles the measurement of resistivity takes depends on a noise threshold (maximum variance of the signal), which may be set up to allow the best quality of the data. We set a medium value of 0.1 for this threshold. If the noise levels are higher, the measurement will take more time to achieve the variance expected.

Dipole-dipole array was used with a distance of 2 m between stainless steel electrodes and maximum length of either 50 m or 100 m (Fig. 1). Data were taken up to 12 m of distance between current and voltage electrodes ( $n = 6$ ). Some of the soundings were placed in plots without the presence of animals at higher topographic positions (background sites: s1, s6, s7) and the others were placed at critical sites such as the traffic area of animals (s2), zones of animal feeding (s3 and s12) and at the surroundings of the lagoon of effluents (s4, s5, s9, s10, s11). Sounding s8 was done near the residence. Experimental data were inverted to obtain 2D models of electrical resistivity of the earth using the DCIP2D code from UBCGIF (2001) following the approach from Oldenburg and Li (1994) and Oldenburg *et al.* (1993). The algorithm finds a model, which reproduces the observed data within the range justified by data uncertainties, trying to avoid under or over fitting. The goal is to find a model that reproduces the earth, based upon data that are contaminated by noise, so the model does not produce predicted data that exactly matches observed data but a model whose data misfit function attains a target value: the number of data (if the errors are supposed to be Gaussian).

To deal with non-uniqueness, of all acceptable models, it computes the one that minimizes the following objective function  $\Phi_m(m, m_0)$  where  $m$  is the final model and  $m_0$  the initial model:

$$\Phi_m(m, m_0) = \alpha_s \iint (m - m_0)^2 dx dz + \iint \left\{ \alpha_x \left[ \frac{\partial(m - m_0)}{\partial x} \right]^2 + \alpha_z \left[ \frac{\partial(m - m_0)}{\partial z} \right]^2 \right\} dx dz$$

and where  $\alpha_s$ ,  $\alpha_x$  and  $\alpha_z$  are adjustable constants that may be selected following previous geological information. In our case, no specific information on the sites was introduced and the parameters were chosen to search a model that varies as little as possible, a model with minimal structure in the two directions, being  $\alpha_x$  and  $\alpha_z$  equal to one (Oldenburg *et al.* 1993; Oldenburg and Li 1994).

A suitable size for the difference between predictions and observations can be determined based on the standard deviation of field data. The assumptions are that errors are Gaussian, independent, with mean zero.

The misfit function between predicted ( $\rho_{ai}^{predicted}$ ) and observed ( $\rho_{ai}^{observed}$ ) data is calculated by

$$\phi = \sum_{i=1}^n \left( \frac{\rho_{ai}^{predicted} - \rho_{ai}^{observed}}{\varepsilon_i} \right)^2$$

where  $\varepsilon_i$  is the experimental error estimated by the resistivity-meter, as the standard deviation of the data obtained from the measurements and  $n$  is the number of data. These errors may be unrealistically low and makes  $\phi$  too high to attain the target misfit, causing some difficulty for the convergence of the inversion as was the case for our measurements. In these cases, an alternative estimation of the errors is recommended as a 5% of the potential measurement at the point plus a base level of 5% of the average value of background potentials ( $n$  max) over the five adjacent points (UBCGIF 2001 (<http://www.eos.ubc.ca/research/ubcgif/iag/tutorials/tutorial-v9.pdf>)).

Then, the inversion consists in minimizing the objective function subject to fitting the data to a specified degree (the number of data if the errors are supposed to be Gaussian).

Analysis of depth of investigation, for which models are still supported by data, was applied following the Oldenburg and Li (1999) approach (i.e., the depth below which surface data are insensitive to the value of resistivity of the Earth). The values of model resistivity at each site were compared with the background site s1, in order to detect low resistivity  $\rho$  (high bulk conductivity  $\sigma$ ) at the non-saturated zone and at groundwater, related with possible leakage of effluents from animal management.

The relative percentage of anomaly in resistivity of the non-saturated zone at each site  $\Delta\rho\%$  was determined as:

$$\Delta\rho\% = \frac{\rho' - \rho_b}{\rho_b} \cdot 100$$

where  $\rho'$  and  $\rho_b$  are the non-saturated zone resistivities at each site and at the background sounding, respectively.

### Groundwater and soil analysis

Groundwater and soil samples were taken at background and the most critical sites, leading the sampling according to previous electrical resistivity models. Physicochemical analyses were carried out in order to test the relationship between soil salinity

(electrical conductivity, ECs) and ion concentrations due to animal waste and bulk conductivity obtained from the inverse of electrical resistivity given by the models.

Groundwater samples were taken from existing wells (see Fig. 1): p1 (mill placed nearby an abandoned drinking trough), p2 (near the milking house), p3 (background mill located upgradient from the milking house) and from wells p4 and p5 (near the residence), all of them at 20 m depth, approximately.

Three wells were drilled to detect free groundwater level and obtain samples from an unconfined aquifer: next to the background site of sounding s1 (well pf1) and, following geoelectrical results, at the most critical sites: next to the lagoon (well pf2) and at the feeding zone (well pf3).

Standard analyses were done: pH, electrical conductivity EC, total dissolved solids (TDS), majority ions ( $\text{Ca}^{2+}$ ,  $\text{Mg}^{2+}$ ,  $\text{Na}^+$ ,  $\text{K}^+$ ,  $\text{Cl}^-$ ), carbonates ( $\text{CO}_3^{2-}$ ), bicarbonates ( $\text{CO}_3\text{H}^-$ ), sulphates ( $\text{SO}_4^{2-}$ ), nitrates ( $\text{NO}_3^-$ ), total alkalinity, total hardness and As. These values were compared with threshold values for animal and human consumption. Correlation between bulk conductivity of the saturated zone and electrical conductivity of groundwater was estimated to test the ERT as a diagnosis of water salinity. Both conductivities are related through the formation factor (Allred *et al.* 2008). Groundwater conductivity was also correlated with ion concentrations to analyse which elements related with animal waste are contributing to increase conductivity.

Soil samples were obtained, from surface up to 1 m depth, representative of horizons 0–20 cm, 20–40 cm, 40–60 cm, 60–80 cm and 80–100 cm, at the background site next to sounding s1 (samples M1) and at the most critical site, which following geophysical results was s3, the feeding zone (samples M2). Analyses of pH, electrical conductivity of the saturated soil paste extract ECs, nitrates, phosphorous, organic matter, total nitrogen, sulphates,  $\text{Ca}^{2+}$ ,  $\text{Mg}^{2+}$ ,  $\text{Na}^+$ ,  $\text{K}^+$  and CEC were performed (Page 1982). Multiple correlation between ECs and ion concentrations was estimated, to analyse which elements contribute to increase ECs.

## RESULTS AND DISCUSSION

### Testing bulk electrical conductivity ( $\sigma$ ) results from ERT with EC obtained from sampling

Figure 2(a) shows the models of 2D electrical resistivity distribution obtained from the inversion of experimental data (estimated error 6.7% average over all the sites). The experimental error decreases to 5% at depths above the depth of investigation (where models are well supported by the data). Pseudosections of observed data and misfit errors are also shown in Fig. 2(b), showing in almost all cases values around 1 for depths above depth of investigation. Misfit is comparable to experimental errors. It must be outlined that conductivity obtained from ERT models is bulk conductivity, at the non-saturated zone and at the saturated zone. It is interesting to analyse its relationship with groundwater conductivity.

### Non-saturated zone

From the model at background site s1, it may be seen that the free groundwater level is about 2 or 3 m depth, in agreement with the measured level at the phreatic well (pf1). The non-saturated zone has a resistivity of  $70 \text{ } \Omega\text{m}$  ( $\sigma = 0.0143 \text{ S/m}^1$ ), the same order of magnitude as the average conductivity of the saturated soil paste extract from samples M1 (ECs =  $0.0072 \text{ S/m}^1$ ).

At the model of site s2 (Fig. 2a), values of decreasing resistivity of the non-saturated zone towards the surroundings of the milking house may be observed, where animals are kept in a corral where superficial runoff of effluents from animal management may have occurred. At s3, resistivity of the non-saturated zone ( $\rho = 8 \text{ } \Omega\text{m}$ ;  $\sigma = 0.1250 \text{ S/m}$ ) is lower than the background site, being the average conductivity of soil ECs (samples M2)  $0.1374 \text{ S/m}$ .

At sites s4 and s5, resistivity of the non-saturated zone is lower than background s1, with the lowest values near the lagoon. This anomaly reaches the saturated zone.

At the NE extreme of the model of site s5 and the NW extreme of s11 near the lagoon, resistivity decreases ( $\sigma = 0.0715 \text{ S/m}$  and  $0.1300 \text{ S/m}$ , for s5 and s11, respectively), which means that conductivity increases ten times the background value. The high conductivity anomaly reaches the sounding depth (6 m). At Fig. 1, the area affected by a flood, during a period of heavy rain in 1994 and 2001, is shown. The lagoon of effluents overflowed mainly towards the eastern part and water seepage may have occurred affecting at least the non-saturated zone. Resistivity models for

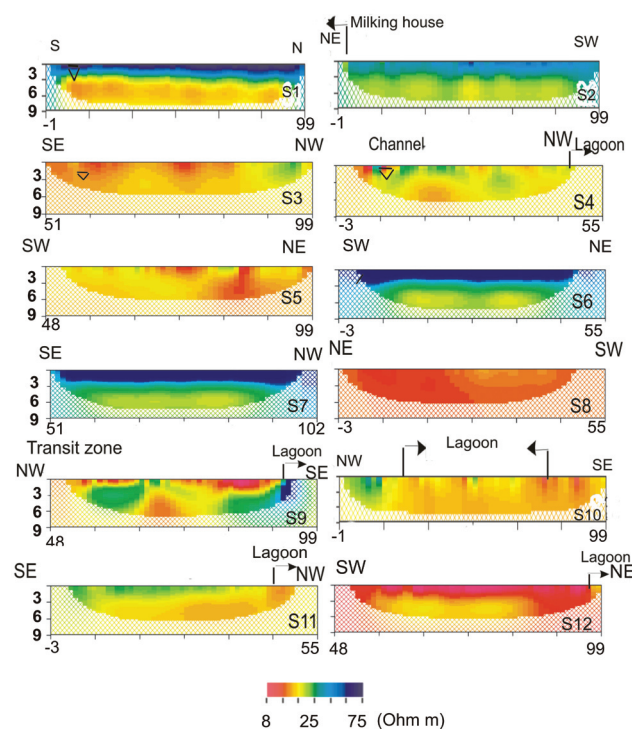


FIGURE 2A

Models of electrical resistivity of the earth in ohm m for each site. The triangle shows free groundwater level. Vertical and horizontal scales in metres.

sites s6 and s7 do not differ very much from the background site, showing that at this pasture plot there are no localized sources of salinity due to animal waste. The model at site s8 is anomalous because this zone was flooded (see Fig. 1) and water remained for a long time in the soil, probably increasing total dissolved salts.

Lower resistivity values of the non-saturated zone are encountered at sounding s10 along the whole width of the lagoon, extending beyond its limit and at s12 ( $\sigma = 0.15$  S/m) below the feeding zone.

The relative percentage of resistivity anomaly  $\Delta\rho\%$  in the non-saturated zone was negligible for models at sites s6 and s7. At the other sites, it varied between  $-60\%$  for sounding s2 and  $-84\%$ , for the feeding zone (s12 and s3), the most critical management unit, while the surroundings of the lagoon showed anomalies around  $-80\%$  (s5, s9 and s10), reaching the saturated zone. The anomalies of electrical conductivity ECs, calculated from soil sampling results (M1 and M2), turned out to be  $-97\%$  at the feeding zone.

The anomalies around the lagoon may also be seen in Fig. 3(a), which is an isoline map of electrical resistivity around the lagoon of effluents, obtained by kriging interpolating values from 2D models, at a depth of 2m. It shows that electrical resistivity decreases from the western part of the lagoon and the lowest values (between 13–18  $\Omega$ m) are encountered at the eastern side of it, just at the area that was overflowed.

### Saturated zone

Table 1 shows physicochemical groundwater properties from samples obtained at phreatic wells (pf1, pf2 and pf3) and at

deeper wells (average 20 m depth). Figure 4 shows the correlation between bulk conductivity  $\sigma_b$ , obtained from ERT models at depth of sample extraction and water conductivity EC (Table 1). Well p1 was not included since there was no nearby sounding to associate with. A good correlation was found ( $R^2 = 0.9$ ) being the slope, the inverse of the formation factor.

At site s3, the ERT model shows lower resistivity (high conductivity) than the background s1, up to 3 m depth for which it may be inferred that free groundwater conductivity is also higher at this site. In fact, free groundwater EC (well pf3, table 1) is 0.2400 S/m, four times the values at well pf1. At well pf2, free groundwater conductivity EC is 0.0660 S/m, higher than the background value.

Figure 3(b) is an isoline map of electrical resistivity of the saturated zone around the lagoon of effluents obtained by kriging, interpolating values from 2D models, at a depth of saturated zone (4 m). The lowest resistivity is found below the feeding area and the flooded zone around the lagoon of effluents.

### Relating electrical conductivity results with major ion concentrations

#### Non-saturated zone. Soil physicochemical analysis

Figure 5 shows the concentration of major ions as a function of depth at the background site (sampling M1) and at the feeding zone (sampling M2). Background samples show similar values of ion concentrations than the ones obtained from regional soil maps (Palazzo *et al.* 2003). Values of Na and pH at the background site M1 coincide with the regional values (INTA 1972) for this soil, where the pH increases with depth due to the increase of concen-

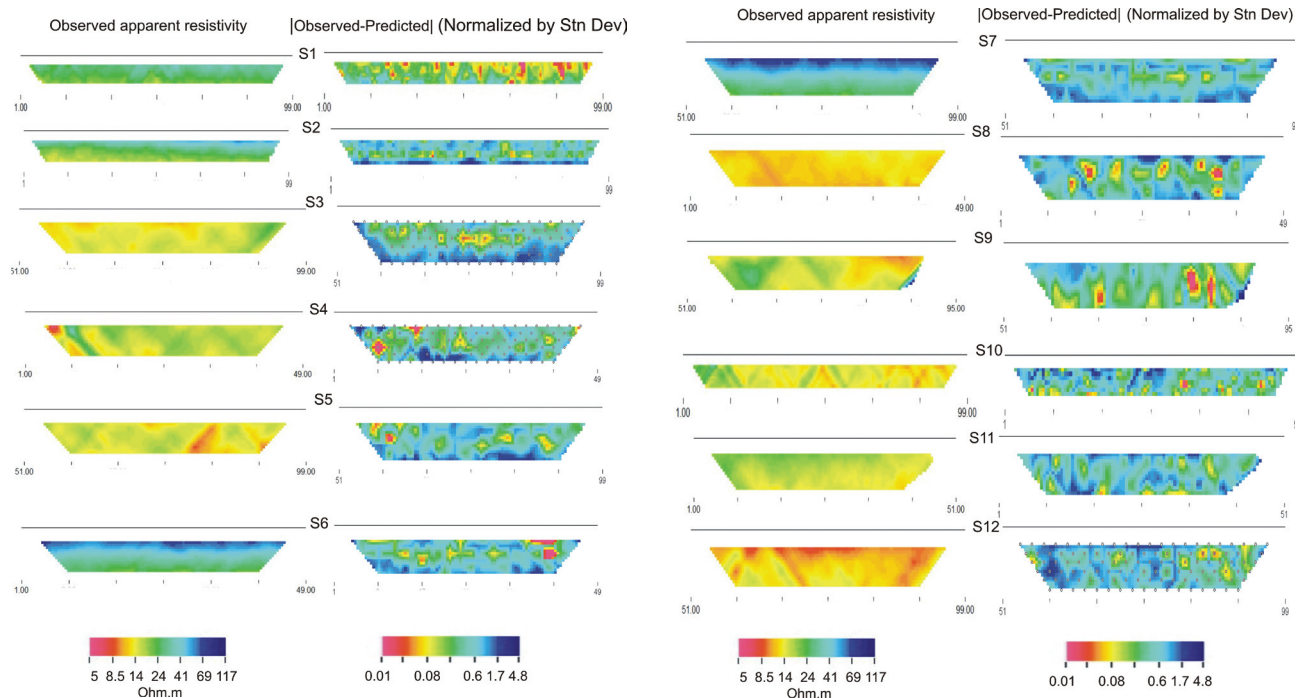


FIGURE 2B

Pseudosections of observed apparent resistivity for each site, together with misfit errors (absolute value of (predicted-observed)/standard deviation).

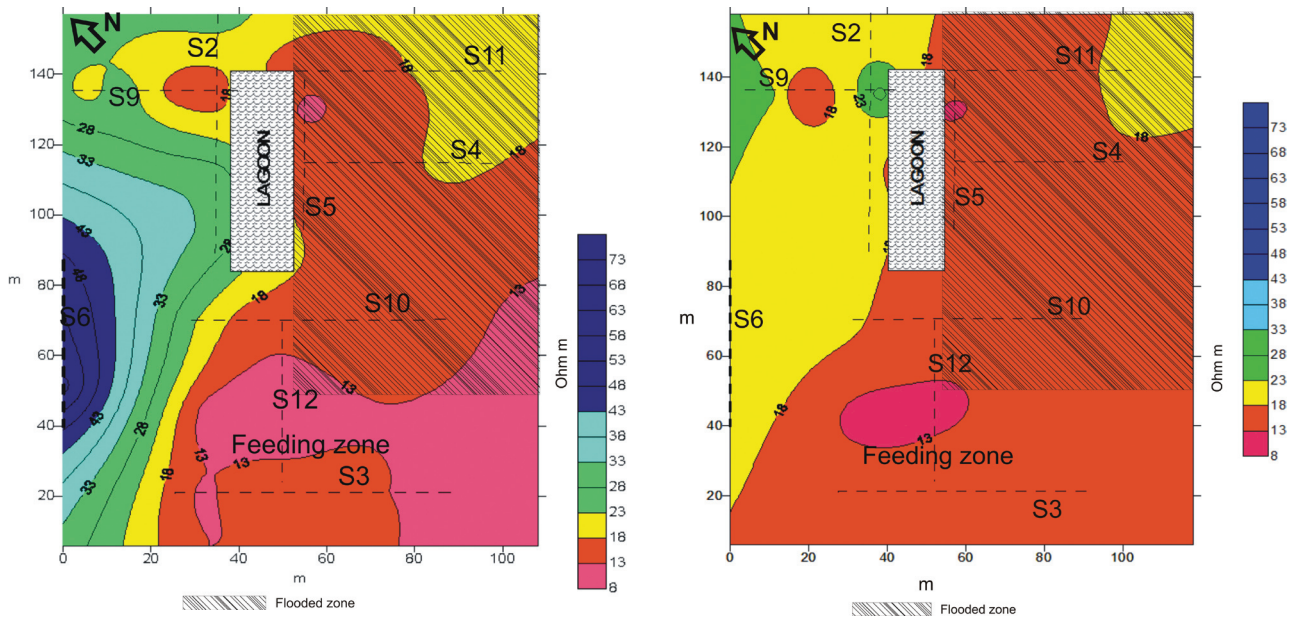


FIGURE 3 Isoline map of electrical resistivity obtained by kriging at the surroundings of the lagoon of effluents. A) At non-saturated zone (2 m depth) and b) at saturated zone (4 m depth).

TABLE 1

Groundwater physicochemical properties obtained from well samples. Depth of groundwater was 20 m approximately for wells p1–p5, while the phreatic level was around 2–3 m at wells pf1–pf3

	Wells								
	p1	p2	p3	p4	p5	pf1	pf2	pf3	
pH	8.01	7.71	7.23	7.4	7.65	6.9	7.1	7.9	
EC (S/m)	0.203	0.135	0.180	0.226	0.329	0.056	0.066	0.240	
TDS (mg/L)	1299	864	1152	1446	2106	370	430	1560	
Ca (ppm)	12	20	22	17.6	12.6	29	36	24	
Mg (ppm)	9.6	20.4	10.8	4.6	12	36	14	45	
Na (ppm)	533	299	355	310	410	50	100	390	
K (ppm)	0.43	0.441	0.505	0.439	0.52	6	10	19	
Cl (ppm)	75	42	42	62	197	26	35	130	
SO4 (ppm)	154.68	0	0	0	0	10	10	60	
Carbonates (ppm)	0	0	0	0	0	0	0	0	
Bicarbonates (ppm)	1174	854	113	1502	1819	380	450	1037	
Nitrates (ppm)	14.46	11.84	3.36	2.21	23.02	35	21	148	
Total alkalinity (ppm)	962	700	912	1231	1550	507	598	1379	
Total hardness (ppm)	70	135	100	63	81	224	149	245	

tration of exchangeable base cations. The carbon content at the upper 40 cm is higher in the background site than the regional values, probably due to the agricultural activity at this site.

Electrical conductivity ECs, sulphates, organic carbon, potassium and nitrate concentrations in samples M2 were substantially higher than M1 up to 60 cm depth. Differences between the two sites decreased at greater depths (60–100cm). These ions are

directly related to the presence of a high recharge of organic matter and as a consequence of animal waste. The phosphorous was much higher at the feeding zone (M2) than the background site up to 100 cm depth and this element was also found in high concentration in water from the lagoon, probably due to its high concentration in animal food. Potassium is an element also present in animal food (forage), whence its concentration in soil

at the feeding zone may be due not only to manure but also to direct contribution of forage. Bulk conductivity  $\sigma_b$  obtained from geoelectrical soundings, organic carbon and ECs values are, at site s3, twice the ones determined at the background site s1. Organic forms are the source of nitrogen which, under the biological processes, can be transformed into inorganic forms as nitrates that can be partly leached. Nitrates are easily dissolved in water, are mobile and can be transported in soil.

A multiple correlation between ECs and concentration of main elements from animal origin showed that nitrates, phospho-

rous and sulphates were positively correlated while organic matter was negatively correlated. Correlation between  $\sigma_b$  and organic matter show different results among literature. Corwin *et al.* (2003) also found positive correlation with nitrates and sulphates and negative correlation with organic matter, at a saline-sodic soil but it was not related with punctual sources of salinity due to animal waste. The manure primarily contributes to carbon and salinity, with a consequent increase in ECs. After some time, the organic matter mineralizes and releases ions.

*Saturated zone. Groundwater analysis*

Figure 6 shows positive correlation between water conductivity EC and concentration of nitrates, sulphates, bicarbonates and chlorides, in samples from a phreatic aquifer (rhombus in the figure) with  $R^2$  above 0.9. No correlation was found for samples from deeper wells.

Free groundwater was classified as sodium bicarbonate for wells pf1 and pf2 while it is chloride sodium bicarbonate for well pf3. This well has much higher values of nitrates, bicarbonates, potassium, chlorides and sulphates than wells pf1 and pf2 and is not acceptable for human consumption nor for irrigation use (CAA 2007). This well coincides with soil samples M2 that also showed an increase of ion concentrations below 80 cm depth. The liberation of carbon dioxide, by the decomposition of organic matter, in contact with water in soil may originate the high concentration of bicarbonates found in groundwater samples. The presence of urea in the

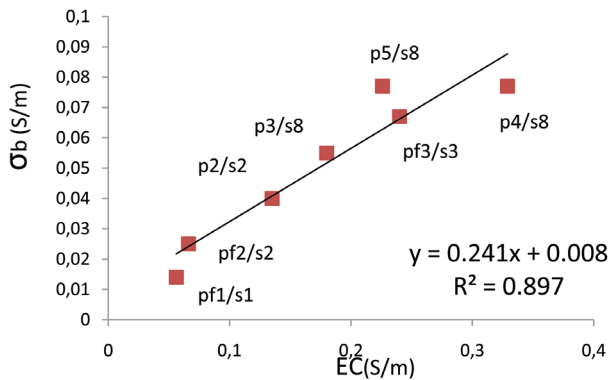


FIGURE 4  
Correlation between bulk conductivity of saturated zone  $\sigma_b$  and water conductivity EC from well samples (labels denote well and near sounding).

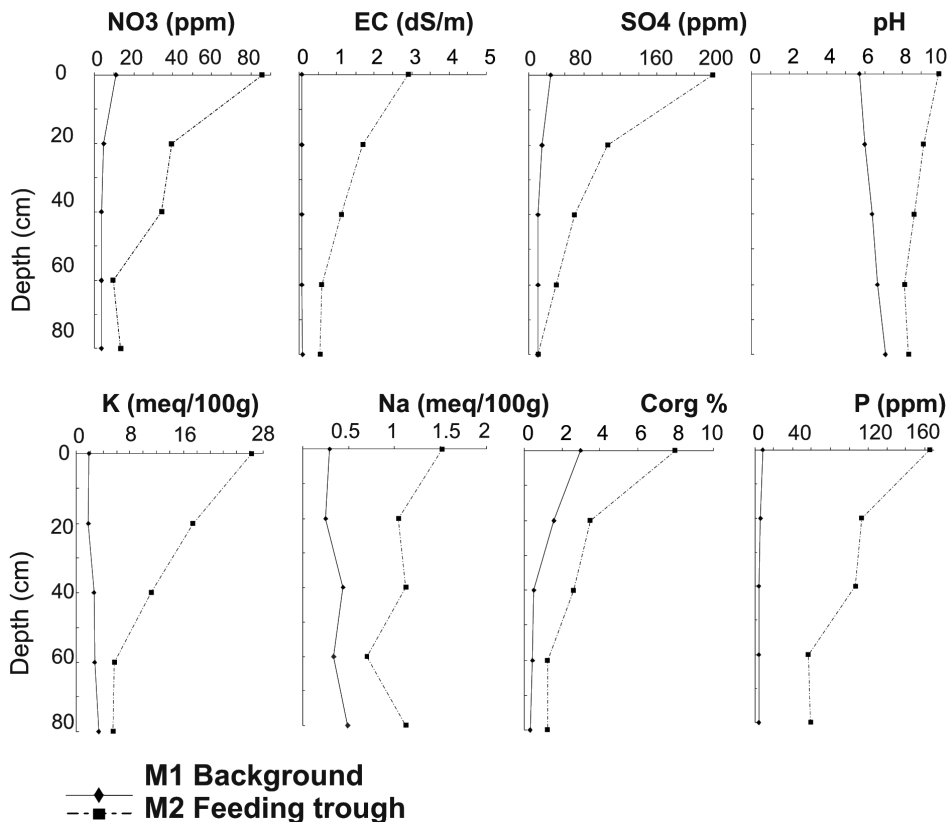


FIGURE 5  
Physicochemical properties of soil as a function of depth for the background site (samples M1) and for the feeding trough location (samples M2).

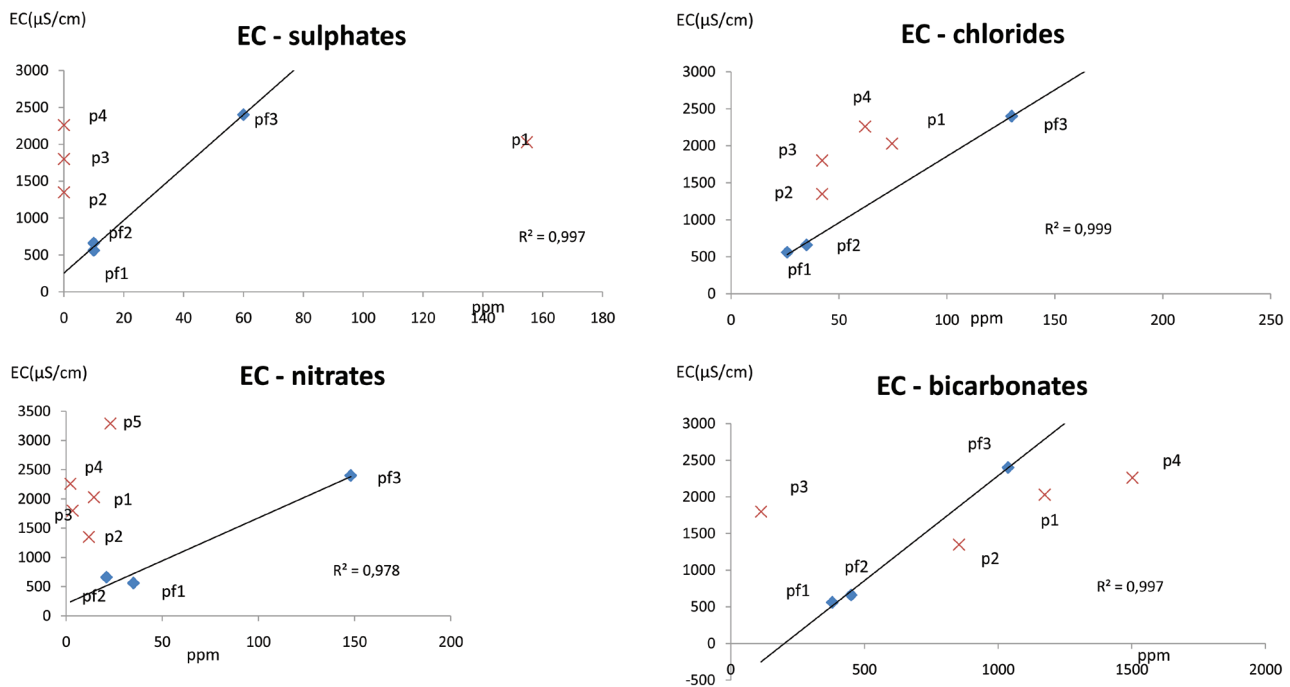


FIGURE 6

Correlation between groundwater conductivity EC and ion concentrations related with animal manure. The cross points correspond to deep wells while the rhombus to phreatic wells (labels denote wells).

manure may also contribute to the increase of pH and alkalinity.

Groundwater at well p5 was classified as chloride sodium bicarbonate and it has the highest values of conductivity, nitrates and chlorides. These characteristics may be due to its location near a septic well that crumbled when flooding occurred. All the other deep wells had water classified as sodium bicarbonate with higher values of electrical conductivity EC, TDS and nitrates compared with background well p3. In particular, well p1 situated by a drinking trough, also had high values of sulphates.

At wells p5 and pf3, EC exceeded the maximum values for human consumption. At well pf3, nitrate concentration is nearly at the maximum value allowed for animal consumption and is over the threshold for human use. Groundwater showed high values of arsenic As (between 0,10–0,20 ppm) from natural origin (Schulz *et al.* 2005), which exceed the threshold for human consumption.

Summarizing, major values of TDS, bicarbonates, nitrates, sulphates, potassium and chlorides were found at sites of high concentration of animals: deep well p1 and feeding zone of well pf3. Even if pf2 is situated near the lagoon, free groundwater quality does not differ too much from the background pf1, which might imply that there is no downward leakage of effluents from the lagoon. However, the eastern side of the lagoon affected by the flood showed soil salinity pointed out by geoelectrical soundings. Water from the lagoon has nitrate concentration of 39 ppm, 856 ppm of potassium and the phosphorous reached a value of 294 ppm.

Consequently, it may be seen that the most critical management unit affected by animal waste is the feeding zone, also used as a cattle confinement plot. At this site and at the surroundings of the lagoon, anomalies of conductivity at the non-saturated zone and saturated zone (phreatic aquifer) encountered with geophysical soundings were well correlated with sampling conductivities at the non-saturated zone (ECs) and saturated zone (EC). The highest contribution to conductivity is correlated with nitrates, sulphates and potassium, in addition with chlorides in groundwater and phosphorous in soils. These elements were also found in water from the lagoon of effluents and are mainly due to urea and animal diets.

In contrast, Losinno *et al.* (2006) did not find anomalies of conductivity in the feeding zone, on a dairy farm at Buenos Aires Province. The soil had finer texture (silty loamy) than our case, with a clay horizon at shallow depth and with similar values of soil saturated hydraulic conductivity around 6 mm/h. On this dairy farm, the location of the feeding trough was periodically changed within all the pasture plots, using a strategy of management of rotation of animal confinement. Alternatively, for our dairy farm at Venado Tuerto, there is a thicker texture, although similar values of soil hydraulic conductivity were encountered. On the other hand, due to the flat topography and the thicker texture, the infiltration process predominates over runoff. Moreover, the risk of groundwater pollution is particularly high in the case of an endorheic basin as in this case. Soil does not have an argilic clay (Bt) horizon near-surface and the feeding zone has a permanent animal

charge, thus this may have favoured leakage of wastes, since the increase of ion concentrations at this management unit are directly or indirectly related with animal origin.

## CONCLUSIONS

Electrical resistivity tomography was sensitive enough to evaluate anomalies in the distribution of electrical resistivity produced by animal waste and management effluents. At the non-saturated zone, high values of bulk electrical conductivity coincide with high conductivity of soil and concentration of phosphorous and potassium. In the saturated zone, bulk conductivity correlated with electrical conductivity of groundwater associated with high concentrations of nitrates, sulphates and chlorides. High pH and alkalinity may also come from urea included in animal waste. An increase in bicarbonates has been observed, which may have an indirect origin from animal waste. The electrical resistivity tomography allowed a quick comparison between different management units of the dairy farm.

The most critical situation is the feeding area, where seepage of effluents was present in the whole soil profile and reached free groundwater. At the surroundings of the lagoon of effluents, where overflow had occurred in the past, geoelectrical results showed that soil and free groundwater had anomalous low resistivity. It may be concluded that on this dairy farm, with a sandy loamy soil, with no presence of a clayey horizon near-surface, sites with high animal charge during a long time or the lagoon of effluents, where an intensive rainy period caused flooding, are localized sources of contamination affecting soil and groundwater.

## ACKNOWLEDGEMENTS

This work was financially supported by the University of Buenos Aires (UBACyT G089). The authors want to thank Ing. Agr. Verónica Charlon for the additional support from the Division Milk Quality and Agroindustry. INTA EEA Rafaela (Santa Fe Province, Argentina) and Ing. Agr. Maria Alejandra Herrero from Veterinary Faculty of UBA for her comments.

## REFERENCES

- Allred B., Daniels J. and Ehsani M. 2008. *Handbook of Agricultural Geophysics*. CRS Press.
- Andriulo A., Nasal C., Amándola C. and Rimatori F. 2003. Impacto de un sistema intensivo de producción de carne vacuna sobre algunas propiedades del suelo y del agua. *Revista de Investigaciones Agrarias* **32**, 27–56 (in Spanish).
- CAA. 2007. Código Alimentario Argentino. Ministerio de Salud y Ambiente. Secretaría de política, regulación y relaciones sanitarias art 982 (Res.Conj SPR yRS y SAGPyA n° 68/2007 y n° 196/2007). [www.anmat.gov.ar](http://www.anmat.gov.ar)
- Corwin D.L., Kaffka S.R., Hopmans J.W., Mori Y., van Groenigen J.W., van Kessel C. *et al.* 2003. Assessment and field scale mapping of soil quality properties of a saline-sodic soil. *Geoderma* **114**, 231–259.
- Drommerhausen D., Radcliffe D., Brune D. and Gunter H. 1995. Electromagnetic conductivity surveys of dairies for groundwater nitrate. *Journal of Environmental Quality* **24**, 1083–1091.
- Fe. República Argentina. Proinsa S.A. Instituto superior de correlación geológica. [http://www.unt.edu.ar/fcsnat/INSUGEO/geologia\\_13/10\\_fili.htm](http://www.unt.edu.ar/fcsnat/INSUGEO/geologia_13/10_fili.htm)
- Filí M.F., Díaz E.L. and Dalla Costa O. A. 1999. Modelo Hidrogeológico Conceptual de la relación entre los acuíferos pampeano y Puelche en un Sector del sur de la Provincia de Santa
- Harter T., Davis H., Mathews M.C. and Meyer R.D. 2002. Shallow groundwater quality on dairy farms with irrigated forage crops. *Journal of Contaminant Hydrology* **55**, 287–315.
- Herrero M.A., Gil S.B., Flores M.C., Sardi G.M. and Orlando A.A. 2006. Nitrogen and phosphorus whole farm balance on dairy farms in Argentina. *In Vet* **8**, 9–21
- Herrero M.A., Iramain M.S., Korol S., Buffoni H. and Flores M. 2002. Calidad de agua y contaminación en tambos de la cuenca lechera de abasto sur, Buenos Aires (Argentina). *Revista Argentina de Producción Animal* **22**, 61–70 (in Spanish).
- IHOBE. 2003. Manual práctico para la investigación de la contaminación del suelo. Sociedad Pública de gestión ambiental. Gobierno Vasco-España.
- INTA. 1972. Instituto Nacional de Tecnología Agropecuaria. Carta de Suelos: Hoja 3363-36. Venado Tuerto. Argentina.
- Losinno B., Sainato C., Malleville H., Aramendi S., Galindo G. and Herrero M.A. 2006. Efectos de la actividad lechera en las propiedades del agua subterránea y del suelo. Actas del XX Congreso Argentino de la Ciencia del Suelo, Salta, Argentina.
- Meju M. 2000. Geoelectrical investigation of old/abandoned, covered landfill sites in urban areas: model development with a genetic diagnosis approach. *Journal of Applied Geophysics* **44**, 115–150.
- Oldenburg D.W. and Li Y. 1994. Inversion of induced polarization data. *Geophysics* **59**, 1327–1341
- Oldenburg D.W. and Li Y. 1999. Estimating depth of investigation in dc resistivity and IP surveys. *Geophysics* **64**, 403–416
- Oldenburg D.W. and Li Y. 1993. Inversion for applied geophysics: A tutorial. UBC-Geophysical Inversion Facility. Department of Earth and Ocean Sciences, University of British Columbia, Vancouver, Canada.
- Oldenburg D.W., McGillivray P.R. and Ellis R.G. 1993. Generalized subspace methods for large-scale inverse problems. *Geophysical Journal International* **114**, 12–20.
- Page A.L., Miller R.H. and Keeney D.R. 1982. *Methods of Soil Analysis. Part 2: Chemical and Microbiological Properties*, 2<sup>nd</sup> edn. ASA-SSSA, Madison, USA.
- Palazzo R., Soza D. and Bernal G. 2003. Recopilación hidrogeológica de la Pcia. de Santa Fe integrada a un GIS para la elaboración de cartografía. Primer Seminario Hispano Latinoamericano sobre Temas Actuales de la Hidrogeología Subterránea.
- Rossi M.M.S. 2004. Materia orgánica: su utilización en la evaluación de la calidad del suelo en distintos ambientes del sur de Santa Fe. Informaciones Agronómicas. IPNI.
- Sainato C., Galindo G., Malleville H. and Herrero M.A. 2006. Diagnóstico de la contaminación en suelo y agua subterránea por actividad ganadera mediante sondeos geoeléctricos en la microcuenca del arroyo Cañete (Pcia. de Bs. As.). *Revista de la Facultad de Agronomía UBA* **26**, 73–82.
- Schulz C., Castro E. and Mariño E. 2005. Presencia de Arsénico en las aguas subterráneas de la Pampa. Acta Taller de Arsénico del IV Congreso Hidrogeológico Argentino. Río Cuarto, Córdoba, Argentina.
- UBCGIF. 2001. University of British Columbia. Geophysical Inversion Facility.
- Ullman J.L. and Mukhtar S. 2007. Impact of dairy housing practices on lagoon effluent characteristics: Implications for nitrogen dynamics and salt accumulation. *Bioresource Technology* **98**, 745–752.